Elements

An International Magazine of Mineralogy, Geochemistry, and Petrology

December 2021
Volume 17, Number 6

ISSN 1811-5209

HEAVY STABLE ISOTOPES: From Crystals to Planets

FRANÇOIS L. H. TISSOT and MAURICIO IBAÑEZ-MEJIA, Guest Editors

Unlocking the Single-Crystal Record of Heavy Stable Isotopes

François L. H. Tissot[1] and Mauricio Ibañez-Mejia[2]

Cathodoluminescence mosaic of a sliced face of the Mud Tank zircon megacryst MTUR1, showing internal oscillatory zoning.

1811-5209/21/0017-0389$2.50 DOI: 10.2138/gselements.17.6.389

Stable isotopes provide deep insights into processes across a wide range of scales, from micron- to cosmic-size systems. Here, we review how continued advances in mass-spectrometry have enabled the analysis of ever-smaller samples and brought the field of heavy stable isotope geochemistry to its next frontier: the single-crystal scale. Accessing this record can be as enlightening as it is challenging. Drawing on novel systematics at different stages of development (from well-established to nascent), we discuss how the isotopes of heavy elements, such as magnesium, iron, zirconium, or uranium, can be used at the single-crystal and subcrystal scales to reconstruct magma thermal histories, crystal growth timescales, or, possibly, magma redox conditions.

Keywords: MC-ICP-MS; diffusion; zircon; iron; zirconium; uranium; stable isotopes

THE SCALES OF ISOTOPE CHEMISTRY

Isotope chemistry is unique among the physical sciences in that the length scales of the questions it aims to answer span more than 17 orders of magnitude. Wondering about the architecture of the early Solar System and its galactic neighborhood (>10^{12} m)? Study the isotopic signatures of meteorites and their constituents. Musing about the age of the Earth or the Moon (~10^6 m)? The radioactive products of short-lived and long-lived parent isotopes in ancient rocks hold the answers. Trying to pinpoint metabolic pathways or identify organ/cellular dysfunction (<10^{-6} m)? Once again, isotope fractionations can result in telltale signatures that the burgeoning field of isotope metallomics is exploring. This remarkable versatility makes isotope chemistry a naturally invasive discipline, which has, in the last few decades, rapidly expanded into numerous fields of Earth and planetary sciences, forensics, archaeology, biology, and, more recently, medical research.

Regardless of their origin, the scale at which isotope effects can be quantified inherently limits the questions that can be investigated. Indeed, to study the processes that shaped a given system one needs to be able to study its components: for example, organs/blood for the human body, minerals for a rock, representative mantle/crust fragments for the Earth, or meteorites for the Solar System (Fig. 1). Technological advances and discoveries are, thus, intimately intertwined in isotope chemistry, with each new generation of instruments enabling scientists to tackle long-standing questions and open new avenues of research, or even entire subfields.

THE INSTRUMENT–DISCOVERY LOOP

To illustrate how innovations and discoveries go hand-in-hand in isotope chemistry, a useful element to consider is uranium (U). It was recognized early on that establishing the relative abundances of the naturally occurring isotopes of U (^{238}U, ^{235}U, and ^{234}U) was necessary for the accurate determination of their respective decay constants, which in turn impacts the reliability of all calculated U–Pb dates. Uranium was, thus, one of the first heavy elements whose isotopic composition was carefully characterized. Using spark-source mass spectrography (an ancestor of mass spectrometry in which separated ion beams are recorded on a photographic plate, and abundances determined using the lines' brightness), two early attempts yielded only upper limits on the abundance of ^{235}U (Fig. 2A). In 1939, Alfred O. Nier reported the first analysis of the isotopic composition of U, with an impressive 1% relative precision on ^{238}U/^{235}U. This analytical *tour-de-force* used a unique mass-spectrometer that Nier developed (Box 1A) and required milligram quantities of uraninite, an almost pure U (88 wt%) compound (Nier 1939). In the 80 years since this seminal work, steady advances in mass spectrom-

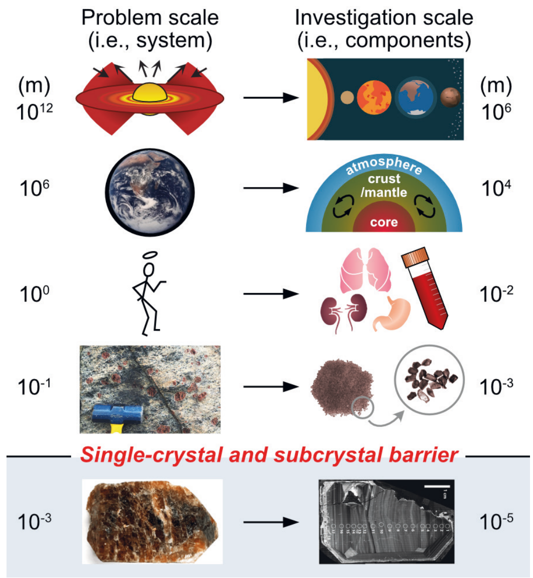

Figure 1 Understanding a system (left), requires investigating its components (right). Isotope analyses of minor elements in single minerals is a burgeoning field that promises insights into magmatic processes.

1 California Institute of Technology
The Isotoparium, Division of Geological and Planetary Sciences
Pasadena, CA 91125, USA
E-mail: tissot@caltech.edu

2 University of Arizona
Department of Geosciences
Tucson, AZ 85721, USA
E-Mail: ibanezm@arizona.edu

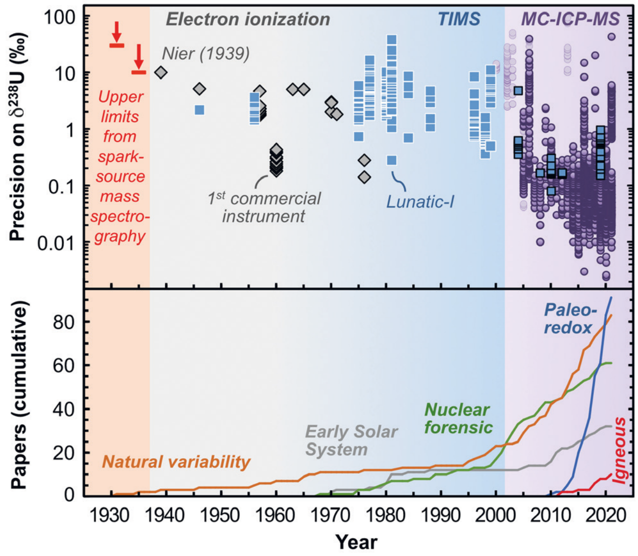

Figure 2 (top) Precision of published δ^{238}U values. Abbreviations: TIMS = thermal ionization mass spectrometry; MC-ICP-MS = multicollector inductively coupled mass spectrometry. (bottom) Cumulative number of papers reporting δ^{238}U, for different subfields. Multicollector instruments (dark rim squares and circles) can resolve small natural δ^{238}U variations, which have become a crucial proxy for oceanic paleoredox reconstructions. Data source: Uranium Isotope Database (www.isotoparium.org/uid).

etry, sample preparation, and chromatographic techniques have enabled the study of ever-smaller samples (Fig. 2A). Today, ^{238}U/^{235}U measurements can be performed with 500× superior precision, using 10^5–10^6 × less U (Tissot et al. 2019), and have expanded to all rock types, fundamentally impacting the study of chronology, Solar System formation, and oceanic paleoredox reconstructions (Andersen et al. 2017).

While the evolution of mass-spectrometers has a rich history (e.g., Sparkman 2006), Box 1 highlights three milestones that have catapulted forward the field of stable isotope geo/cosmochemistry. First is the appearance in the 1970s of digital TIMS (thermal ionization mass spectrometer) instruments (e.g., Lunatic-I, Wasserburg et al. 1969). Looking at a mass spectrometer today, one easily forgets that, for decades, these instruments had to be run by hand, whether to adjust the strength of the electric/magnetic fields or to read signal outputs on physical strip charts. The introduction of digitally controlled instruments represented a quantum leap forward, enabling for the first time: (1) rapid field scanning; (2) programmable (and, thus, truly repeatable) analyses; and (3) rapid and automated data collection and integration. By increasing the amount of time spent on sample analysis, and by eliminating systematic biases from the data processing workflow and beam instabilities, digital instruments were able to achieve significantly higher precision and sensitivity over their analog counterparts. Second, is the introduction, in the 1980s, of multicollector arrays. By enabling the simultaneous detection of all isotopes of interests, multicollection alleviates virtually all concerns of beam instability: all ion beams respond in unison to instabilities, little affecting the measured isotope ratios. Digital (single-, and later, multi-collector) mass spectrometers rapidly became the norm and permitted fundamental advances in all branches of isotope geo/cosmochemistry, including, for example, the study of stellar contributions to the protoplanetary disk, early Solar System chronology, lunar formation, Quaternary geology and climatology, nuclear forensics, and human evolution.

Box 1 Mass Spectrometers Used for Heavy Stable Isotope Analyses

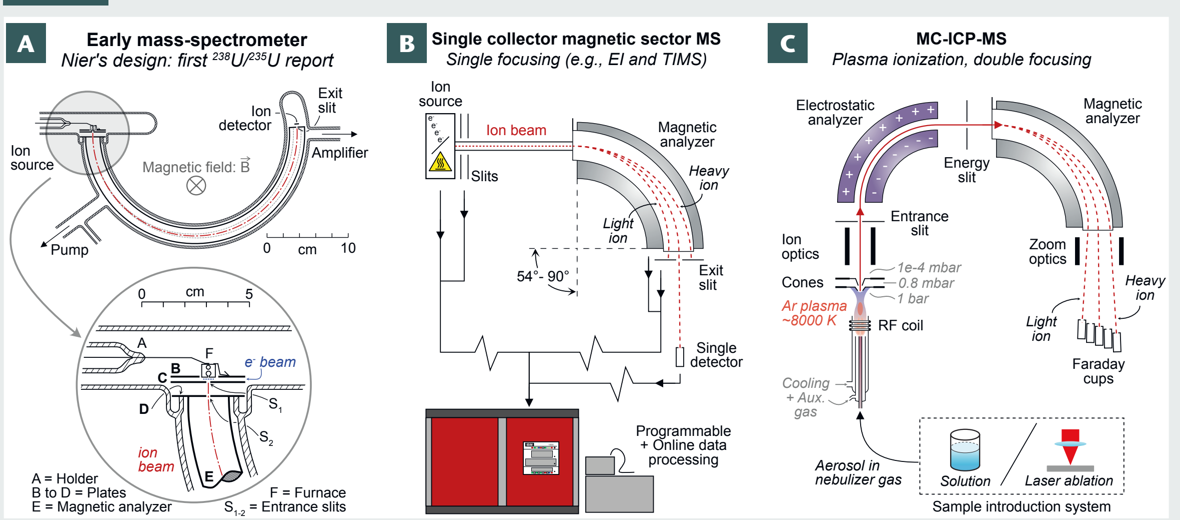

Schematic depiction of three generations of mass spectrometer. (**A**) Early mass spectrometer. (**B**) Single-collector magnetic sector mass spectrometer. (**C**) Multicollector inductively coupled plasma mass spectrometer (MC-ICP-MS).

Similarities: In all instruments, ions produced in the source are accelerated through an electric potential, focused into a beam (using lenses with variable potential and/or slits), and sent into a magnetic analyzer that separates ions as a function of their mass-to-charge ratio. For a given magnetic field, lighter ions are deflected more than heavier ions.

Differences: In Nier's 1939 prototype (**A**), the samples were loaded and heated in a miniature furnace to produce a vapor (gas-source), which was then ionized by an electron beam (electron ionization). In TIMS (**B**), sample solution drops are loaded onto a filament and dried to a salt (typically a chloride or a nitrate). An electric current running through the filament thermally ionizes the sample, producing an ion beam with small kinetic energy spread. In MC-ICP-MS (**C**), the sample is introduced as an aerosol into an argon plasma, where it is evaporated, vaporized, atomized, and ionized. An interface (typically two cones with aligned apertures of decreasing sizes), allows transfer of the ions from the plasma (at atmospheric pressure) to the vacuum of the mass-spectrometer's front end (~10^{-4} mbar). Due to the large range of kinetic energy of the ions, an additional, electrostatic, analyzer is used to focus ions of different energies. In MC-ICP-MS (and modern TIMS), the ion beams deflected by the magnet are simultaneously measured using multiple detectors aligned on the focal plane of the ion beam.

A notable feature of the scientific avenues explored using heavy isotopes, even after the advent of digital mass spectrometers, is that the vast majority of them relied on the characterization of mass-independent signatures: (1) the quantification of (e.g., $^{87}Rb \rightarrow ^{87}Sr$, $^{147}Sm \rightarrow ^{143}Nd$, U-series, $^{26}Al \rightarrow ^{26}Mg$) or the search for (e.g., $^{107}Pd \rightarrow ^{107}Ag$, $^{247}Cm \rightarrow ^{235}U$) radiogenic ingrowth of daughter isotopes; and (2) the characterization of nucleosynthetic anomalies in Solar System materials (e.g., Ca, Ti, Sr, Ba, Nd, Sm).

Because mass-dependent isotope fractionations decrease with both increasing temperature and nuclide mass, so-called "stable" isotopic variations in heavy elements, even in low-temperature environments, were expected to be (and in most cases, are) of limited magnitude (per mil to sub–per mil). For most elements, resolving such small isotopic effects, and, more importantly, turning them into quantitative proxies of physico-chemical processes, took a third instrumental revolution: the introduction of MC-ICP-MS (multicollector inductively coupled plasma mass spectrometer) instruments in the 1990s (Box 1C) (e.g., Albarède and Beard 2004). The ICP-MS instruments ionize the samples using argon plasma introduced either as aerosols (i.e., micro droplets from sample solutions, or as solid particulates from laser ablation) or, less commonly, as a gas. The high temperatures inside the plasma (~8,000 K) achieve extremely efficient ionization, even for the most refractory elements (e.g., tungsten). The smooth drift of instrumental mass bias with time, combined with a rapid sample introduction, provides the ability to monitor mass fractionation externally, by simple standard bracketing, and/or internally, by comparison to the mass bias of another element with similar mass (i.e., element doping) or artificially enriched isotopes of the same elements (i.e., isotope spiking). The drastic improvement in analytical precision offered by this technology is visible in Figure 2A, when pioneering studies leveraging MC-ICP-MS instruments and synthetic ^{233}U–^{236}U spike isotopes resolved natural variations in $^{238}U/^{235}U$ (Stirling et al. 2007; Weyer et al. 2008) by achieving precisions as low as 0.10‰ to 0.04‰ while using only a few 10s to 100s of nanograms of U. Since then, refinements in sample introduction, ion transmission, electronics stability, and methodologies have steadily improved the achievable precision. Today, $^{238}U/^{235}U$ variations have not only been documented in a plethora of terrestrial and extraterrestrial materials, but $^{238}U/^{235}U$ in marine sediments (mainly carbonates) has become, arguably, the most widely used proxy of ocean paleoredox conditions (Zhang et al. 2020).

Although the history of each isotope systematic is unique, the general picture depicted by U holds true for other heavy elements, and the entire field of "nontraditional" stable isotopes, which emerged in the 2000s as MC-ICP-MS instruments started to be adopted worldwide, has since rapidly expanded to most of the periodic table.

HEAVY STABLE ISOTOPES AND THE SINGLE-CRYSTAL LENS

As more and more stable isotope systems are now the subject of sustained attention, the major limiting factor for future avenues of exploration will become the amount of sample needed for high-precision analysis. Even though for many systems MC-ICP-MS instruments enable high-precision work with only 1–10 mg of sample, a common barrier remains for most heavy stable isotopes: analysis at the single-crystal and subcrystal scale. The incentives to reach past these barriers are obvious. First, to understand a system and the processes that shaped it, one needs to be able to study the components of this system individually (Fig. 1). A useful parallel can be drawn with geochronology, where single-grain analyses have long been possible owing to the large isotopic effects stemming from radioactive decay. Dating using the U-Pb system used to require such large quantities of lead that pooled zircon fractions (up to 1000s of crystals) were digested and analyzed together as a single "sample". The chronological constraints obtained were useful but provided only an aggregated average of the sample's history. As single-grain geochronology methods were developed, the spread in dates obtained from individual grains transformed our understanding of natural processes, enabling us, among other things, to reconstruct sediment provenance, as well as precisely determining the timescales of mass extinctions and the cooling histories of magma chambers (e.g. Schoene 2014).

Being able to study the isotopic signature of single minerals and their internal zonation is also critical for accessing the detrital mineral record of Earth's evolution. In studies of the early Earth (the first ~500 My), detrital zircons are the only known lithic witnesses remaining. Therefore, our capacity to extract qualitative and quantitative information from these unique grains is crucial to understanding the Hadean Eon, which presumably saw the waning of the extraterrestrial bombardment, the emergence of life, and the establishment of continents (Harrison 2020).

For heavy elements, which tend to display small stable isotope variability, the analytical challenges associated with breaching through the single-crystal barrier are inversely correlated with elemental abundances. For elements present in trace quantities in minerals, this barrier is still insurmountable, because the absolute amount of element contained in a single crystal is simply too small to yield high-precision data, even when using the most sensitive instruments currently at our disposal (see Box 2). On the other hand, a growing body of work is studying isotopic variability of major constituents in minerals of interest: Fe–Mg in olivine [$(Fe,Mg)_2SiO_4$], Ti in ilmenite ($FeTiO_3$), and Zr in zircon ($ZrSiO_4$) and baddeleyite (ZrO_2) (e.g., Sio et al. 2013; Johnson et al. 2019; Ibañez-Mejia and Tissot 2019). Single-grain analysis of elements present in only minor abundances (between ~100 ppm and 1 wt%) represents the current frontier of the field.

Box 2 SAMPLING THE SUBGRAIN SCALE

***Micromilling*:** Samples subgrain domains ~50–300 µm wide. The powders recovered can be processed through wet chemistry and analyzed at the highest levels of precision.

***Laser ablation MC-ICP-MS*:** Provides finer spatial resolution than micromilling, with spots ~20–80 µm wide and ~10–30 µm deep, and higher sample throughput than solution work. This comes at a cost in precision, due to the lack of sample purification (e.g., matrix effects, limited ion detection for low abundance elements).

***Multicollector secondary ion mass spectrometry (MC-SIMS)*:** Produces spots as small as 50–500 nm wide and submicron in depth. As with laser ablation, data accuracy requires matrix matching between standards and samples (see Sio et al. 2013 for comparison of the above three methods for Fe isotopes).

Other methods, such as resonance ionization mass spectrometry (RIMS) or atom probe tomography, show promise for measuring isotope ratios of the heavy elements at finer (nanometric) spatial resolution.

As discussed by Watkins and Antonelli (2021 this issue), elemental and isotopic gradients in single mineral grains testify to the processes at play during crystal growth and subsolidus cooling, as well as concurrent changes in magma composition. The successive growth layers of a mineral can, thus, act as a record of their crystallization pathway, cooling history, and the evolving characteristics of their parental magma (e.g., composition, redox, *T*, amount of differentiation). To illustrate the potential of single-crystal and subcrystal heavy stable isotopes inves-

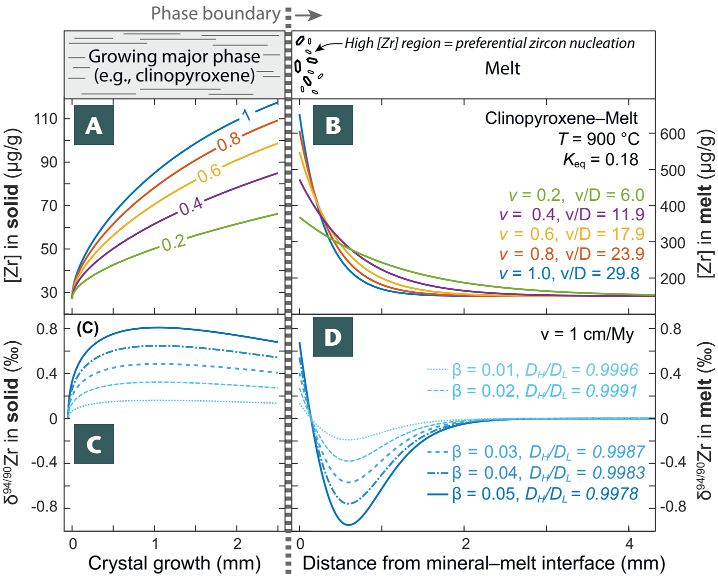

FIGURE 3 The growth of a major rock-forming phase with a low (<1) K_{eq} for Zr (e.g., clinopyroxene) leads to preferential zircon nucleation in high-[Zr] and $\delta^{94/90}$Zr diffusive boundary layers in the melt. (TOP) Profile of [Zr] developed in the growing solid (**A**), and the silicate melt (**B**), assuming growth velocities, v, of 0.2–1.0 cm/My. (BOTTOM) Profiles of $\delta^{94/90}$Zr developed in the growing solid (**C**), and the melt (**D**), due to kinetic (diffusive) isotopic fractionation in the liquid driven by clinopyroxene crystallization. The effect of variable β at a constant solid growth velocity (1 cm/My) are shown (dashed lines). See Watkins and Antonelli (2021 this issue) for definitions of D, D_H, D_L, and β. MODIFIED AND EXPANDED FROM MÉHEUT ET AL. (2021).

tigations we highlight below three applications using systems at different stages of development and discuss the constraints that these novel tools place on high-T processes.

PUSHING PAST THE SINGLE-CRYSTAL FRONTIER: MAJOR RESULTS AND PROMISES

The Well-Established Fe–Mg Interdiffusion Probe

Discerning between mineral zoning established during crystal growth versus that resulting from subsolidus diffusion has been a long-standing challenge in the field of geospeedometry. Indeed, in diffusion-based geospeedometry, elemental zonations in rock-forming minerals such as olivine, plagioclase, and pyroxene are used to reconstruct the thermal history of geological systems (e.g., Costa et al. 2020). A fundamental difficulty of this approach is deconvolving elemental profiles resulting from crystal growth in an evolving magma from those developed by volume diffusion (e.g., during cooling, while the temperature is still high enough to drive chemical diffusion). Theoretically, isotopes can tease apart these end-member scenarios. Consider an olivine growing in a magma of evolving composition. If the olivine grows under equilibrium conditions, the amount of Fe and Mg it will uptake (i.e., its Fe/(Fe + Mg) ratio) will be purely controlled by (1) the Fe and Mg concentration in the surrounding melt, and (2) the equilibrium partition coefficients of Fe and Mg in olivine. Assuming a constant Fe and Mg isotope composition for the melt (i.e., Fe and Mg uptake in the growing olivine and other minerals does not result in any significant isotopic fractionation), the final olivine grain will display Fe and Mg elemental zoning, but no isotope variations. On the other hand, an initially homogeneous olivine crystal (i.e., no Fe–Mg zoning) affected by interdiffusion of Fe and Mg during subsolidus cooling would develop both elemental and isotopic zoning. The faster diffusion of the light isotopes of Fe (inward) and Mg (outward) would then lead to diagnostic, and mirroring, isotopic patterns for Fe and Mg (Fig. 5 in Watkins and Antonelli 2021 this issue). Although intermediate scenarios between these end-members are, of course, likely to occur, for instance where concurrent growth and diffusion are happening, a diffusion-driven, negative correlation between Fe and Mg isotopes would still be expected.

This hypothesis was the motivation for a series of laser ablation studies (see Watkins and Antonelli 2021 this issue) that targeted olivine crystals from the Kilauea Iki lava lake (Hawaii, USA), some intraplate volcanic systems, and even Martian meteorites, which have collectively established the applicability of Fe–Mg stable isotope studies within single crystals to reconstruct the thermal histories of the grains (and, by extension, their parental magma). In particular, Sio and Dauphas (2017) showed, through an inverse modeling exercise, that although numerous time–temperature (t–T) paths yield acceptable fits to the Fe–Mg chemical zoning in olivine grains from the Kilauea Iki lava lake, only a minor subset provide a good fit to the isotopic profiles. More importantly, t–T paths that fit the isotope data also are the closest match to the known cooling history of the sample, making Fe and Mg isotope analysis in single olivine crystals a powerful geospeedometer.

The Budding Zr System: Expectations vs. Data

Several isotope systems, most notably molybdenum (Mo), titanium (Ti), calcium (Ca), and zirconium (Zr) isotopes, have recently become the focus of attention as tracers of igneous processes. These provide us with an opportunity to see how tools in early stages of development evolve. In particular, we will focus on Zr isotopes, for which single-grain and subgrain studies are available.

Elemental Zr is a widely used tracer of magmatic differentiation. Both a refractory lithophile and a moderately incompatible transition metal, Zr concentration generally increases as differentiation progresses in silicate melts. Zirconium also plays a key role in the development of accessory phases such as zircon (tetragonal $ZrSiO_4$) and baddeleyite (monoclinic ZrO_2), which are fundamental to the study of geologic time and Earth's crustal evolution. As Zr-rich accessory phases are a major Zr sink, early studies investigating Zr stable isotopes (e.g., Ibañez-Mejia and Tissot 2019; Inglis et al. 2019) were motivated by the possibility that equilibrium isotope fractionation during zircon formation would lead to Zr isotope variations (expressed as $\delta^{94/90}$Zr) during magmatic differentiation. The rationale behind a nonzero solid–melt isotope fractionation factor was the higher coordination of Zr in zircon (8-fold), and baddeleyite (7-fold) than in silicate melts (6-fold), and the differences in bond lengths. In this framework, zircon-fertile magmas would see their $\delta^{94/90}$Zr shifting away from less evolved ones (e.g., primary basalts), and Zr isotopes were seen as a potential tool to constrain the chemical evolution of the crust/mantle through geologic time.

Far from these simple expectations, data obtained on bulk rocks, single zircon/baddeleyite crystals, and profiles across single zircons grains, have yielded conflicting results, with inferred zircon–melt fractionation factors varying not only in magnitude but also in direction (from +1‰ to −0.5‰) (review in Méheut et al. 2021). What's more, most isotope fractionation factors derived from natural samples are, at least, one order of magnitude larger than those predicted by ab initio calculations (~ ±0.05‰ at 800 °C) (Méheut et al. 2021), indicating that equilibrium, mass-dependent (i.e., vibrational) isotope effects are unlikely to control Zr isotope fractionation in most of the settings studied. At present, the $\delta^{94/90}$Zr variability observed in zircon seems to most likely stem from diffusive effects (FIG. 3), with isotope fractionation factors of apparently opposite signs testifying to the conditions under which zircon growth took place. For instance, in a melt of homogeneous Zr concentration

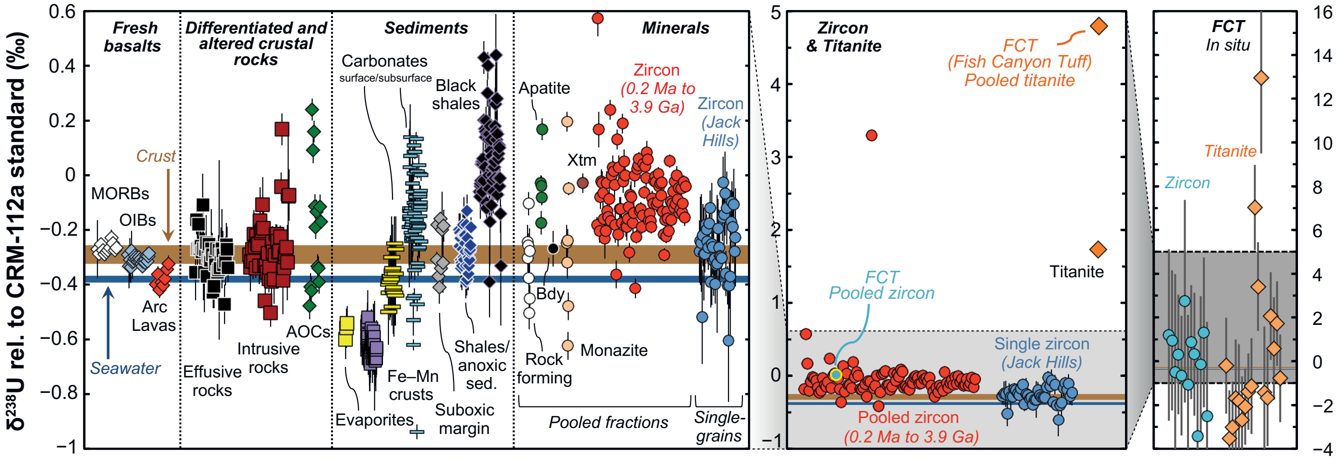

FIGURE 4 The $\delta^{238}U$ (±95% CI) for representative igneous and modern sedimentary rocks, and minerals. Variability increases from fresh basalts, to differentiated crustal rocks, to igneous minerals (pooled fractions and single-zircon grains). Modern sediments, where $\delta^{238}U$ variations are routinely and quantitatively interpreted as redox signatures, are shown for comparison. Titanite shows extreme fractionations. Abbreviations: MORB = mid-ocean ridge basalt; OIB = ocean island basalt; AOC = altered oceanic crust; Bdy = baddeleyite; Xtm = xenotime. DATA: TISSOT AND DAUPHAS (2015) (+REFS THEREIN); LIVERMORE ET AL. (2018); TISSOT ET AL. (2018, 2019); YAMAMOTO ET AL. (2021).

reaching zircon saturation, a growing zircon will deplete its immediate surrounding (i.e., melt) in Zr, thereby developing a chemical gradient. Diffusion of Zr from the melt towards the growing solid would result in lighter compositions near the core of a growing crystal and progressively heavier compositions towards the rim (e.g., Watson and Müller 2009). This model can readily explain the internal $\delta^{94/90}Zr$ profiles observed to date in zoned zircon crystals from silicate magmas (Guo et al. 2020).

Taken at face value, the extreme $\delta^{94/90}Zr$ variability (from ~+1‰ to −4‰) (Ibañez-Mejia and Tissot 2019) in zircon and baddeleyite grains from the mafic magma of the Duluth Gabbro (Minnesota, USA), and mean positive value relative to the bulk rock, would require zircon crystallization to fractionate $^{94}Zr/^{90}Zr$ ratios by ~1‰, a value so large that it is unlikely to be due to equilibrium effects alone. A more likely explanation is that the growth of major phases in which Zr is moderately to very incompatible would result in Zr build-up at the mineral–melt interface, creating a chemical gradient and a diffusive boundary layer (DBL) (FIG. 3) (Méheut et al. 2021). As the DBL becomes enriched in Zr, faster diffusion of lighter isotopes away from the DBL would render this region isotopically heavy towards the mineral–melt interface, and isotopically light away from the interface (FIG. 3). In this scenario, zircon nucleation / growth would preferentially occur near the major phase–melt interface, where [Zr] and $\delta^{94/90}Zr$ are high.

The Zr isotope system, initially expected to become a simple proxy for magmatic differentiation, appears instead to provide insight into kinetic (diffusive) processes during magmatic evolution. As such, the Zr isotope systematics in Zr-rich phases, and also in major phases (e.g., clinopyroxene) (FIG. 3), might prove more useful as tracers of crystallization timescales, petrologic processes, and thermal histories. More work is needed to fully understand the applicability of the system.

A Promising Terra Incognita: The U Isotope System

The uranium isotope system ($^{238}U/^{235}U$), which has been extensively studied in the context of oceanic paleoredox reconstructions and ore deposit formation, has also garnered attention in igneous samples for its potential as a tracer of Soret (thermal) diffusion (Telus et al. 2012), subduction and sediment recycling (e.g., Andersen et al. 2015), or for the impact that $^{238}U/^{235}U$ variations have on U–Pb and Pb–Pb ages (Hiess et al. 2012; Tissot et al. 2017; Livermore et al. 2018). These initial investigations revealed striking features in the $\delta^{238}U$ ($^{238}U/^{235}U$ expressed in delta notation) record of igneous rocks and minerals (FIG. 4), including (1) a wider range of variability in differentiated crustal rocks (~0.60‰) than in fresh basalts (~0.20‰); (2) large $\delta^{238}U$ variations (up to 3.7‰) between pooled-fractions (hundreds to thousands of single crystals) of zircon from different localities and age; (3) $\delta^{238}U$ variations between pooled-fractions of zircon and other accessory minerals (up to 4.8‰ between titanite and zircon) derived from the same parental melts. Collectively, these data clearly indicate the existence of significant mineral-specific U isotope fractionations and/or kinetic isotope fractionations (similar to Zr) occurring at magmatic temperatures. Yet, the exact mechanisms behind U isotope fractionation in magmatic settings remain almost entirely unconstrained.

At present, identifying the underlying processes driving the observed fractionations in natural samples is impossible due to the dearth of data on U coordination, valence, and speciation in accessory minerals (Hanchar 1999), and due to the paucity of single-crystal $\delta^{238}U$ data in these phases. Indeed, a common feature to the aforementioned investigations is that they approach the study of igneous samples and magmatic differentiation at the bulk level (bulk rock or pooled mineral fractions). The typical abundance of U in zircon and other accessory minerals (e.g., apatite, monazite, titanite) is only ~1,000 ppm (or less), resulting in absolute amounts of U contained by individual crystals so small (≤ single-digit ng) that they were traditionally regarded as insufficient to allow for precise $^{238}U/^{235}U$ determinations (Hiess et al. 2012; Livermore et al. 2018).

A first breach of the single-crystal barrier for $\delta^{238}U$ was recently made by Tissot et al. (2019), who showed that state-of-the-art MC-ICP-MS combined with careful sample handling could render high-precision U isotope analysis of single-zircon not only possible but also broadly applicable. This is true even in concert with the chemical abrasion treatment used for high-precision U–Pb and Pb–Pb geochronology, and could enable improvements in precision and accuracy of U–Pb and Pb–Pb dates, more accurate U-series disequilibria corrections to U–Pb data, and a reevaluation of U decay constants. Investigation of Hadean/Archean single-zircon grains from the Jack Hills (Australia) revealed resolvable $\delta^{238}U$ variations (up to 0.60‰), consistent with the existence of mineral-specific U isotope fractionation effects. Moreover, the average $\delta^{238}U$ values in the Jack Hills zircons is identical to that of chondrites, but lower than the average values of multigrain zircon fractions spanning the post-Eoarchean history, suggesting either (i) an influence of source materials with higher $\delta^{238}U$ in younger rocks, or (ii) a change in mantle redox conditions sometime after the Eoarchean, allowing the expression of a stronger zircon–melt U isotope fractionation than those observed in older zircons (Fig. 4). Even more recently, Yamamoto et al. (2021) showed that per mil precision $\delta^{238}U$ determination on U-rich accessory minerals was possible with laser ablation MC-ICP-MS and high resistance (10^{13} ohm) amplifiers. These authors not only confirmed the large $\delta^{238}U$ variations observed by Hiess et al. (2012) in titanite from the Fish Canyon Tuff (Colorado, USA), but were also able to demonstrate extreme grain-to-grain variability, from −3.5‰ ± 2.2‰ to +13.1‰ ± 3.4‰. The magnitude of these effects almost certainly indicates a kinetic origin.

The U isotopic systematics of igneous rocks in general, and single crystals in particular, is an exciting *terra incognita*. Turning this potential into a reliable probe to study igneous systems will require efforts on multiple fronts to elucidate the drivers of $\delta^{238}U$ variations in single crystals (Fig. 4). These drivers include (1) synchrotron X-ray spectroscopy (e.g., EXAFS, XANES) investigations to address the cruel lack of data on the bonding environment and valence state of U in minerals; (2) coordinated microtextural, compositional, and isotopic investigations of accessory phases (zircon, titanite, apatite, baddeleyite) from rock samples with well-constrained ages and magmatic origins (e.g., reduced vs. oxidized), to contextualize $\delta^{238}U$ data; (3) ab initio calculations and zircon growth experiments to calibrate the dependency of isotope fractionation to parameters such as oxygen fugacity, temperature, or magma composition; (4) the search for potential correlations between zircon $^{238}U/^{235}U$ ratios and other tracers of source and/or magmatic evolution. By constraining the relationship between the characteristics of the host rock, host mineral, U crystal chemistry/bonding environments, and $\delta^{238}U$ of the grains, such work would provide a robust interpretative framework for U isotope effects in natural accessory phases and bulk samples. Once understood, intercrystal, intermineral and interrock $^{238}U/^{235}U$ variations could become powerful tools for studying magmatic evolution, provenance, redox, and/or composition.

ACKNOWLEDGMENTS

This work was supported by NSF-EAR grants 1824002 (to FLHT), 2131632 and 2131643 (to MIM), and a Packard Fellowship and Caltech start-up funds to FLHT. We thank reviewers M. Andersen, B. Bourdon, J. Davies, and J.-F. Wotzlaw, as well as editors R. Harrison and J. Rosso for constructive reviews that helped improve the manuscript.

REFERENCES

Albarède F, Beard B (2004) Analytical methods for non-traditional isotopes. Reviews in Mineralogy and Geochemistry 55: 113-152, doi: 10.2138/gsrmg.55.1.113

Andersen MB and 5 coauthors (2015) The terrestrial uranium isotope cycle. Nature 517: 356-359, doi: 10.1038/nature14062

Andersen MB, Stirling CH, Weyer S (2017) Uranium isotope fractionation. Reviews in Mineralogy and Geochemistry 82: 799-850, doi: 10.2138/rmg.2017.82.19

Costa F, Shea T, Ubide T (2020) Diffusion chronometry and the timescales of magmatic processes. Nature Reviews: Earth & Environment 1: 201-214, doi: 10.1038/s43017-020-0038-x

Guo J-L and 6 coauthors (2020) Significant Zr isotope variations in single zircon grains recording magma evolution history. Proceedings of the National Academy of Sciences USA 117: 21125-21131, doi: 10.1073/pnas.2002053117

Hanchar JM (1999) Spectroscopic techniques applied to uranium in minerals. Reviews in Mineralogy 38: 499-519

Harrison TM (2020) Hadean Earth. Springer International Publishing, 291 pp, doi: 10.1007/978-3-030-46687-9

Hiess J, Condon DJ, McLean N, Noble SR (2012) $^{238}U/^{235}U$ systematics in terrestrial uranium-bearing minerals. Science 335: 1610-1614, doi: 10.1126/science.1215507

Ibañez-Mejia M, Tissot FLH (2019) Extreme Zr stable isotope fractionation during magmatic fractional crystallization. Science Advances 5, eaax8648, doi: 10.1126/sciadv.aax8648

Inglis EC and 8 coauthors (2019) Isotopic fractionation of zirconium during magmatic differentiation and the stable isotope composition of the silicate Earth. Geochimica et Cosmochimica Acta 250: 311-323, doi: 10.1016/j.gca.2019.02.010

Johnson AC and 7 coauthors (2019) Titanium isotopic fractionation in Kilauea Iki lava lake driven by oxide crystallization. Geochimica et Cosmochimica Acta 264: 180-190, doi: 10.1016/j.gca.2019.08.022

Livermore BD, Connelly JN, Moynier F, Bizzarro M (2018) Evaluating the robustness of a consensus $^{238}U/^{235}U$ value for U-Pb geochronology. Geochimica et Cosmochimica Acta 237: 171-183, doi: 10.1016/j.gca.2018.06.014

Méheut M, Ibañez-Mejia M, Tissot FLH (2021) Drivers of zirconium isotope fractionation in Zr-bearing phases and melts: the roles of vibrational, nuclear field shift and diffusive effects. Geochimica et Cosmochimica Acta 292: 217-234, doi: 10.1016/j.gca.2020.09.028

Nier AO (1939) The isotopic constitution of uranium and the half-lives of the uranium isotopes. Physical Review 55: 150-153, doi: 10.1103/PhysRev.55.150

Schoene B (2014) U–Th–Pb geochronology. In: Turekian HDHK (ed) Treatise on Geochemistry, volume 4 (Second Edition). Elsevier, Oxford, pp 341-378, doi: 10.1016/B978-0-08-095975-7.00310-7

Sio CKI, Dauphas N (2017) Thermal and crystallization histories of magmatic bodies by Monte Carlo inversion of Mg-Fe isotopic profiles in olivine. Geology 45: 67-70, doi: 10.1130/G38056.1

Sio CKI and 5 coauthors (2013) Discerning crystal growth from diffusion profiles in zoned olivine by in situ Mg–Fe isotopic analyses. Geochimica et Cosmochimica Acta 123: 302-321, doi: 10.1016/j.gca.2013.06.008

Sparkman OD (2006) Mass spectrometry: overview and history. In: Meyers RA (ed) Encyclopedia of Analytical Chemistry. John Wiley & Sons, Ltd, Chichester, doi: 10.1002/9780470027318.a6001

Stirling CH, Andersen MB, Potter E-K, Halliday AN (2007) Low-temperature isotopic fractionation of uranium. Earth and Planetary Science Letters 264: 208-225, doi: 10.1016/j.epsl.2007.09.019

Telus M and 7 coauthors (2012) Iron, zinc, magnesium and uranium isotopic fractionation during continental crust differentiation: the tale from migmatites, granitoids, and pegmatites. Geochimica et Cosmochimica Acta 97: 247-265, doi: 10.1016/j.gca.2012.08.024

Tissot FLH, Dauphas N (2015) Uranium isotopic compositions of the crust and ocean: age corrections, U budget and global extent of modern anoxia. Geochimica et Cosmochimica Acta 167: 113-143, doi: 10.1016/j.gca.2015.06.034

Tissot FLH, Dauphas N, Grove TL (2017) Distinct $^{238}U/^{235}U$ ratios and REE patterns in plutonic and volcanic angrites: geochronologic implications and evidence for U isotope fractionation during magmatic processes. Geochimica et Cosmochimica Acta 213: 593-617, doi: 10.1016/j.gca.2017.06.045

Tissot FLH and 7 coauthors (2018) Controls of eustasy and diagenesis on the $^{238}U/^{235}U$ of carbonates and evolution of the seawater ($^{234}U/^{238}U$) during the last 1.4 Myr. Geochimica et Cosmochimica Acta 242: 233-265, doi: 10.1016/j.gca.2018.08.022

Tissot FLH and 6 coauthors (2019) $^{238}U/^{235}U$ measurement in single-zircon crystals: implications for the Hadean environment, magmatic differentiation and geochronology. Journal of Analytical Atomic Spectrometry 34: 2035-2052, doi: 10.1039/C9JA00205G

Wasserburg GJ, Papanastassiou DA, Nenow EV, Bauman CA (1969) A programmable magnetic field mass spectrometer with on-line data processing. Review of Scientific Instruments 40: 288-295, doi: 10.1063/1.1683921

Watkins JM, Antonelli MA (2021) Beyond equilibrium: kinetic isotope fractionation in high-*T* environments. Elements 17: 383-388

Watson EB, Müller T (2009) Non-equilibrium isotopic and elemental fractionation during diffusion-controlled crystal growth under static and dynamic conditions. Chemical Geology 267: 111-124, doi: 10.1016/j.chemgeo.2008.10.036

Weyer S and 5 coauthors (2008) Natural fractionation of $^{238}U/^{235}U$. Geochimica et Cosmochimica Acta 72: 345-359, doi: 10.1016/j.gca.2007.11.012

Yamamoto K, Asanuma H, Takahashi H, Hirata T (2021) In situ isotopic analysis of uranium using a new data acquisition protocol for 10^{13} ohm Faraday amplifiers. Journal of Analytical Atomic Spectrometry 36: 668-675, doi: 10.1039/D0JA00498G

Zhang F and 14 coauthors (2020) Uranium isotopes in marine carbonates as a global ocean paleoredox proxy: a critical review. Geochimica et Cosmochimica Acta 287: 27-49, doi: 10.1016/j.gca.2020.05.011 ■